



Contents lists available at ScienceDirect

Nuclear Inst. and Methods in Physics Research, A

journal homepage: www.elsevier.com/locate/nima

Development of LSI for a new kind of photon-counting computed tomography using multipixel photon counters

Makoto Arimoto^{a,*}, Hayato Morita^a, Kazuya Fujieda^a, Takuya Maruhashi^a, Jun Kataoka^a, Hideo Nitta^b, Hirokazu Ikeda^c

^a Research Institute for Science and Engineering, Waseda University, 3-4-1, Ohkubo, Shinjuku, Tokyo, 169-8555, Japan

^b Hitachi Metals Ltd, Osaka 618-0013, Japan

^c Institute of Space and Astronautical Science (ISAS), 3-1-1 Yoshinodai, Sagami-hara, Kanagawa, 229-8510, Japan

ARTICLE INFO

Keywords:

X-ray CT
MPPC
LSI
Low-dose
Multicolor

ABSTRACT

X-ray imaging with computed tomography (CT) is widely used for nondestructive imaging of the interior of the human body. In the next decade, photon-counting X-ray CT is expected to reduce the dose needed and enable multicolor imaging. Recently, we proposed a novel photon-counting method that uses a multipixel photon counter (MPPC), with a significantly high signal gain ($\sim 10^6$) and fast temporal response (a few nanoseconds), combined with a high-speed scintillator. To realize photon-counting CT imaging in a wide area irradiated by an extremely high X-ray flux (10^6 - 10^7 Hz/mm²), a multichannel MPPC system is required. Thus, we developed a large-scale integrated circuit (LSI) with ultrafast signal-processing capability for use with a 16-channel MPPC. The developed LSI can extract a pulse current from an MPPC array with a large detector capacitance (~ 200 pF) by utilizing an electrical circuit with low input impedance. The LSI offers a high photon count rate above 25 MHz/pixel with noise equal to 1.7 μ A for a dynamic range of ~ 1.3 mA and an energy resolution of 32 % (FWHM) at 60 keV, thereby enabling ultrafast multicolor CT imaging.

© 2017 Elsevier B.V. All rights reserved.

1. Introduction

X-ray computed tomography (CT) is one of the most widely used methods for nondestructive imaging of the interior of the human body. However, conventional X-ray CT has several disadvantages: (1) the required radiation dose is significantly high (~ 10 mSv for one set of CT scans), and (2) different materials with the same CT values (e.g., linear attenuation coefficient) cannot be distinguished since the obtained image is monochromatic due to the use by conventional CT of photodiodes (PDs) that are incapable of signal amplification. Because PDs have large dark currents, many X-ray photons within a short period are required as input. However, in such a case, individual X-ray photons cannot be detected and the output signal is a continuous current that lacks energy information. To overcome these challenges, we proposed a photon-counting X-ray CT system [1] that utilizes a high-speed scintillator combined with a multipixel photon counter (MPPC) that has a significantly high internal gain ($\sim 10^6$) and an extremely fast temporal response. We demonstrated that our system can perform multicolor X-ray CT and drastically reduce the number of X-ray photons

required for X-ray CT by a factor of ~ 100 , thereby offering great potential for low-dose CT imaging.

Similar photon-counting CT systems that use cadmium telluride (CdTe) or cadmium zinc telluride (CZT) have been proposed [2–4]. CdTe and CZT have superior energy resolution compared with scintillation detectors and are advantageous for multicolor imaging such as “K-edge imaging” that utilizes the X-ray characteristic of a K-absorption edge. However, because of the slow carrier mobility of CdTe and CZT, the pixel size needed to tolerate a high X-ray rate would be much smaller than that of typical CT systems ($\sim 1 \times 1$ mm²/pixel). Thus, the number of pixels needed would be extremely large, making CdTe and CZT unrealistic for clinical use and making our MPPC system beneficial for a future CT system.

In our previous study [1], the proposed photon-counting method utilized a single MPPC and a yttrium aluminum perovskite (YAP) scintillator with a fast decay time of ~ 25 ns. A multichannel MPPC system for a large detection area and realistic applications is needed.

* Corresponding author.

E-mail address: m.arimoto@aoni.waseda.jp (M. Arimoto).

<https://doi.org/10.1016/j.nima.2017.11.031>

Received 20 September 2017; Received in revised form 1 November 2017; Accepted 8 November 2017

Available online xxx

0168-9002/© 2017 Elsevier B.V. All rights reserved.

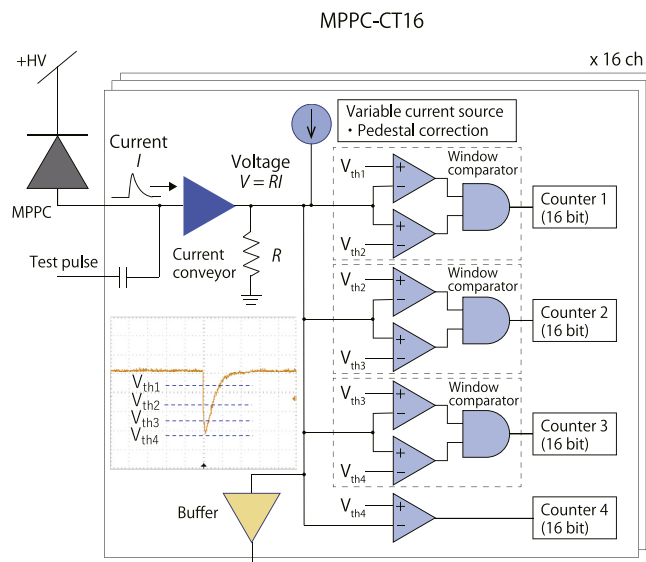


Fig. 1. Schematic diagram of the signal processing by MPPC-CT16.

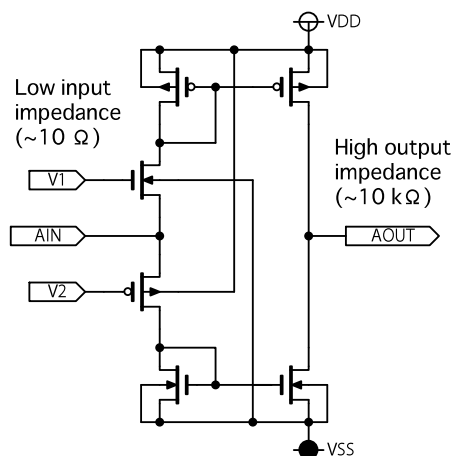


Fig. 2. Electrical circuit of the current conveyor used in the MPPC-CT16.

Thus, we have developed a new LSI, called MPPC-CT16, that performs ultrafast analog and digital signal processing for a 16-channel MPPC.

2. Overview of an MPPC-CT16

An MPPC-CT16 has two basic functions, i.e., analog signal processing and digital signal processing with 16 channels. A schematic diagram of

Table 1
Specifications for the MPPC-CT16.

Number of channels	16
Maximum dynamic range	0 – 4 mA*
Number of energy thresholds	4
Countable range	> 25 MHz/pixel
Power rail	±1.65 V
Power consumption	~230 mW
Foundry	TSMC

* $R = 0.25 \text{ k}\Omega$

both functions is presented in Fig. 1. A pulse current I from an MPPC goes to the resistor R via a current conveyor and is converted to a voltage signal ($V = IR$). The output voltage signal is processed using three window comparators and a normal comparator with four threshold levels (V_{th1} , V_{th2} , V_{th3} and V_{th4}) and is converted to digital output in four counters that provide the number of pulse counts. The pulse height of the output signal differentiated by the four thresholds provides information on the X-ray photon energy, which enables multicolor X-ray CT to be performed. To correct the variation in the pedestal levels of the channels caused by manufacturing variations, we implemented a variable current source whereby the current value for each channel is determined by the control registers in each channel.

For analog processing, the LSI needs to capture the pulse current from an MPPC quickly (i.e., within tens of nanoseconds) to reserve the original pulse shape. However, because MPPCs have a large detector capacitance ($\sim 200 \text{ pF}$), ordinary preamplifiers with extremely high input impedance cannot be used. To obtain the desired fast response of an input amplifier, we used a current conveyor, the electrical circuit of which is illustrated in Fig. 2. The current conveyor has considerably low input impedance ($\sim 10 \Omega$) and significantly high output impedance ($\sim 10 \text{ k}\Omega$). Its superior performance provides high-speed response within tens of nanoseconds and large voltage output. The output voltage is obtained via the resistor R , the value of which can be 0.25, 0.5, or 1 k Ω . For this study, we used $R = 1 \text{ k}\Omega$, which is suitable for the dynamic range determined by the light yield of the scintillator and the gain of the MPPC.

3. Specifications of MPPC-CT16

Fig. 3 shows the layout of the MPPC-CT16 and Table 1 presents its specifications. The MPPC-CT16 was designed and fabricated on a $0.35 \mu\text{m}$ complementary metal–oxide–semiconductor (CMOS) processor with four-metal and poly-insulator-poly (PIP) options, and assembled in a ceramic package of 160 pins.

4. Performance

To operate the MPPC-CT16 and evaluate its performance, we utilized an analog and digital interface board (PCI-7833R, National Instruments) with a reconfigurable field-programmable gate array (FPGA) (LabVIEW FPGA, National Instruments). The LabVIEW FPGA controls the register configuration and reads out the restored number of detected pulse

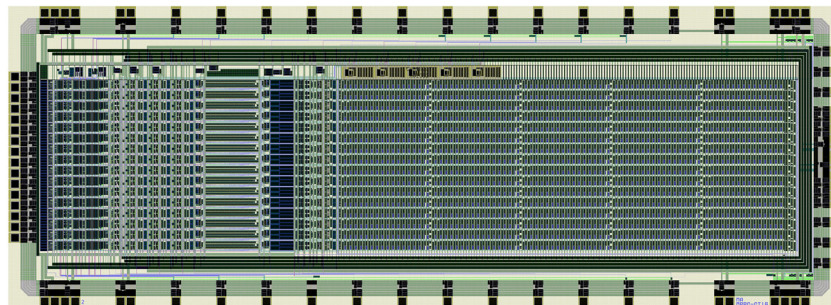


Fig. 3. Layout of a $9.4 \times 3.4\text{-mm}^2$ MPPC-CT16.

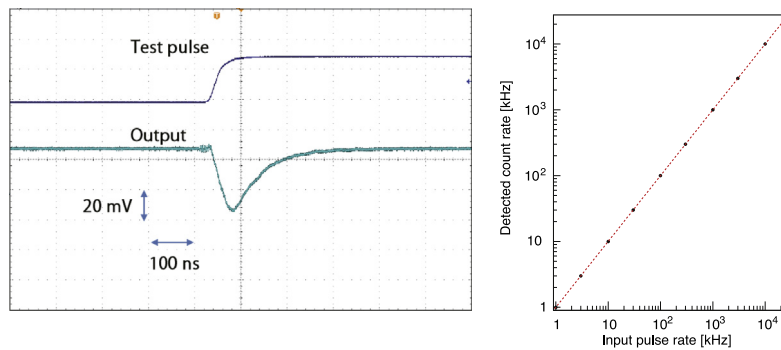


Fig. 4. Left: Output signal of the current conveyor using a test pulse. Right: Input pulse rate versus detected count rate using test pulses up to 25 MHz. The dashed line represents $y = x$.

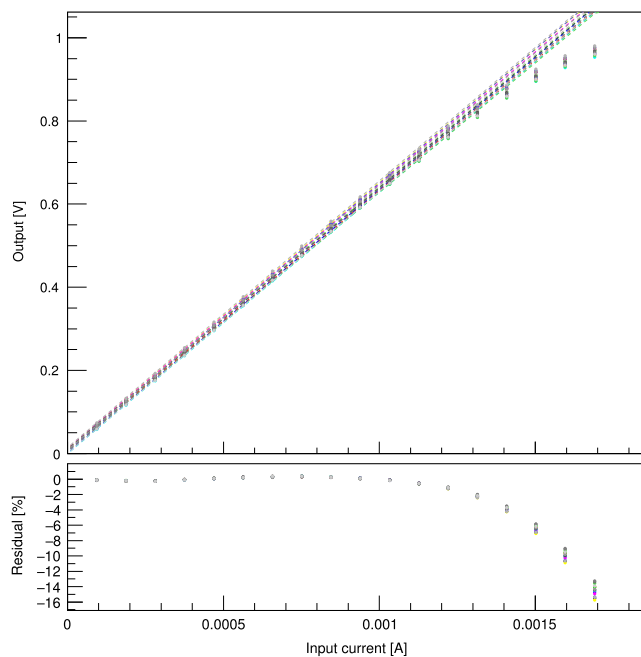


Fig. 5. Top: Linearity performance between the input current and output voltage at a 220-pF load for every channel of the MPPC-CT16. The dashed lines represent the best-fitting linear function. Bottom: Residuals between the data points and the best-fitting functions.

counts. Our data consists of $10 \text{ bits} \times 4 \text{ thresholds} \times 16 \text{ channels} = 640 \text{ bits}$. The data are read out with 12.5-MHz clock via serial-link and the readout time is $\sim 50 \mu\text{s}$. Considering that a typical frame rate is $\sim 1 \text{ kHz}$ or less in the experiment, the readout time is negligible compared with X-ray exposure time.

4.1. Temporal response

To investigate the tolerance of the MPPC-CT16 for extremely high count rates, we fed high-speed charges into the MPPC-CT16 using test pulses from a function generator (AFG-2025, GW Instek). The fast temporal response was confirmed as shown in Fig. 4(left), although the observed waveform was distorted by the buffer amplifier, which has limited performance at high frequency. Fig. 4(right) shows a relationship between the input pulse rate and the detected count rate, and represents that the MPPC-CT16 can count input pulses that have a frequency $> 25 \text{ MHz/pixel}$, thereby confirming that when combined with a scintillator, the MPPC-CT16 is capable of counting all pulse signals from the MPPCs, considering that a complete pulse is $\sim 100 \text{ ns}$.

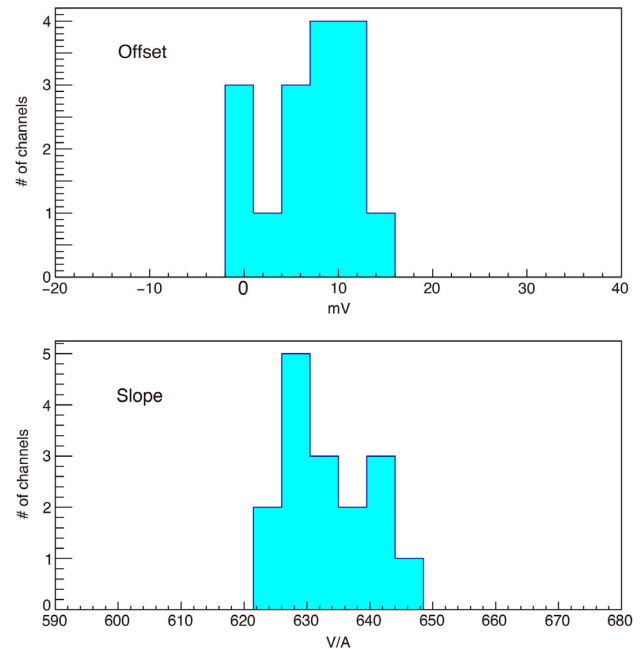


Fig. 6. Top: Offset distribution of the fitted linear function; $7.3 \pm 4.4 \text{ (std) mV}$. Bottom: Slope distribution; $633 \pm 6 \text{ (std) V/A}$.

4.2. Linearity of signal and noise

We evaluated the linearity between the input current and the output voltage using a test-pulse signal, where the current was calculated by considering the rise time and the pulse height of the input square wave. Fig. 5 shows the measured result for every channel, where a 220-pF signal load, a typical MPPC detector capacitance, was used. The results show a good linear relationship for an input current up to $\sim 1.3 \text{ mA}$. For an input current $> 1.3 \text{ mA}$, the output voltage becomes saturated. In the input current range of 0–1.3 mA (which corresponds to the output voltage range 0–0.8 V), the integral non-linearity is estimated to be 1.7% for an average of 16 channels. Fig. 6 shows the distributions of the signal offset and the slope for every channel after correcting the pedestal variations. The slope is $633 \Omega \pm 6 \Omega$ [standard deviation (std)] which is a good uniformity. The signal offset ranges from 0 to $\sim 15 \text{ mV}$, which indicates that the maximal energy difference of effective thresholds is $\sim 3 \text{ keV}$, an almost negligible variation considering the obtained energy resolution [$\sim 120 \text{ mV}$ at full width at half maximum (FWHM)], as discussed in Section 4.4.

The inherent LSI noise was estimated by obtaining the S-curve, which was measured by conducting a threshold scan via a fine shift of the

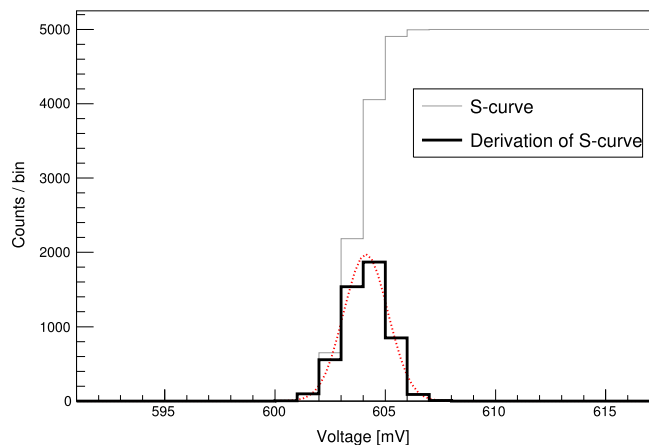


Fig. 7. S-curve scan measured using a fine shift of the threshold voltage. The LSI noise corresponds to the width of the Gaussian distribution obtained by differentiating the S-curve. The dashed line represents the best-fit function.

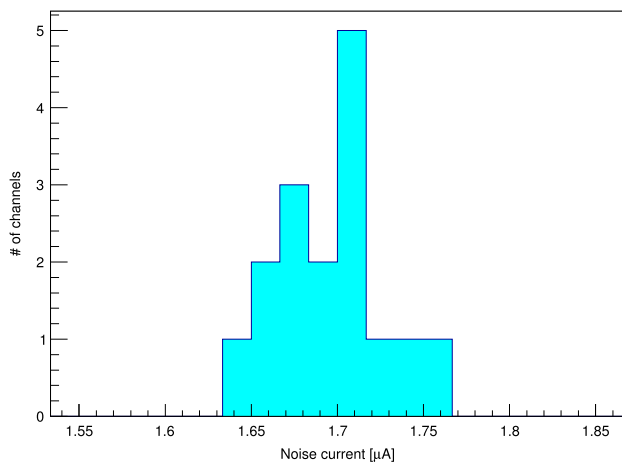


Fig. 8. INOISE distribution of $1.70 \mu\text{A} \pm 0.03 \mu\text{A}$ (std) under a 220-pF load for every channel of the MPPC-CT16.

threshold voltage ($\Delta V = 1 \text{ mV}$), as illustrated in Fig. 7. By differentiating the S-curve, we obtained the Gaussian distribution, the width of which corresponds to the LSI noise. The measured noise was converted to the equivalent input noise current (INOISE). The INOISE distribution at a 220-pF load is shown in Fig. 8 and was estimated to be typically $1.7 \mu\text{A}$ at the root mean square (rms). The corresponding voltage noise was $\sim 1 \text{ mV}$, indicating that the LSI noise was extremely low and completely negligible with respect to other uncertainties such as the energy resolution.

4.3. Dependence on capacitance

The distortion of the shape of the MPPC pulse is dependent on the detector capacitance. For MPPCs with a large detector capacitance to be used appropriately, the dependence should be evaluated. The dependence of the slope and INOISE on the detector capacitance is shown in Fig. 9. The detector capacitance contributes to the distortion of the MPPC pulse shape and significantly reduces the output voltage (e.g., a $\sim 400\text{-pF}$ load reduces the output by a factor of two compared to the output with a 0-pF load). Correspondingly, the INOISE increases when the detector capacitance is larger. The voltage noise is almost constant at $\sim 1 \text{ mV}$ (rms) for different detector capacitances. Since the detector capacitances significantly affect the performance, such as the signal gain (e.g., slope in Fig. 9), careful calibration is needed to obtain accurate energy information.

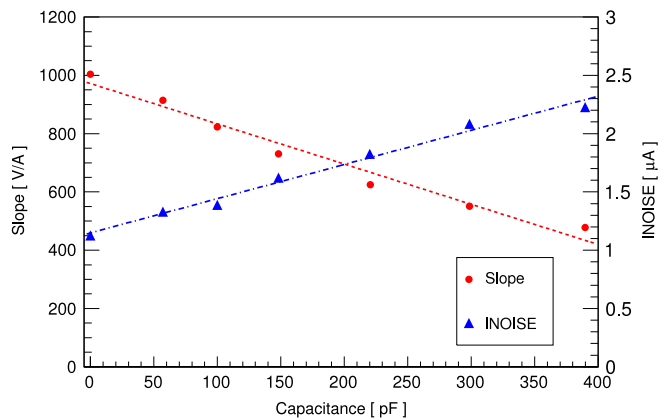


Fig. 9. Slope and INOISE for different load capacitances. The best-fit linear function for Slope is $972 \Omega - 1.4 \Omega/\text{pF}$ (dashed line) and that for INOISE is $1.15 \mu\text{A} + 0.003 \mu\text{A}/\text{pF}$ (dashed-dotted line).

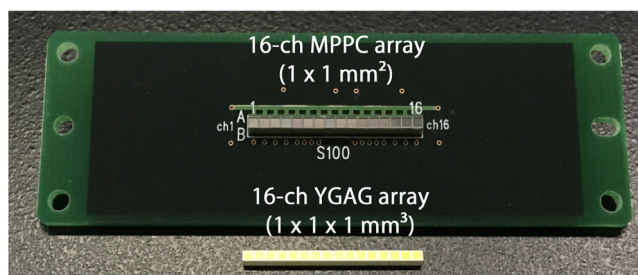


Fig. 10. The 16-channel MPPC array and the 16-channel YGAG scintillator array.

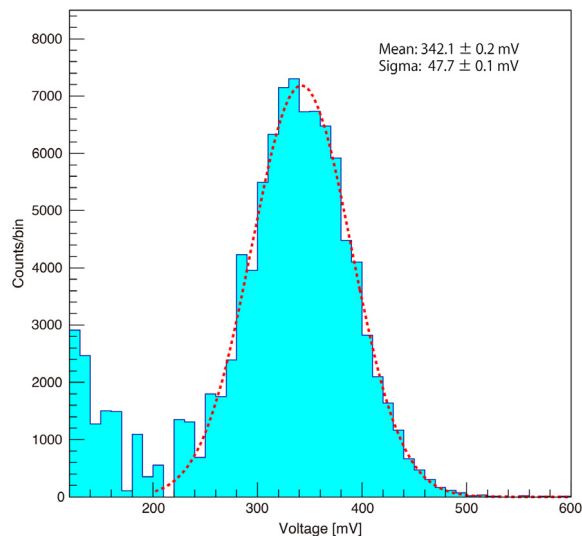


Fig. 11. Representative energy spectrum of 60 keV obtained with a 16-channel MPPC array and a 16-channel YGAG scintillator array using ^{241}Am as the radiation source. The dashed line represents the best-fitting Gaussian function.

4.4. Energy spectra with MPPC array

We obtained energy spectra using a 16-channel MPPC array (Hamamatsu Photonics), a 16-channel yttrium–gadolinium–aluminum–gallium garnet (YGAG) scintillator array (Hitachi Metals), and the MPPC-CT16. The MPPC array comprised of 16 MPPCs, each with an area of $1 \times 1 \text{ mm}^2$ and $25\text{-}\mu\text{m}$ pitch. The scintillator array comprised of 16 YGAGs, where each YGAG was $1 \times 1 \times 1 \text{ mm}^3$ and had a decay time

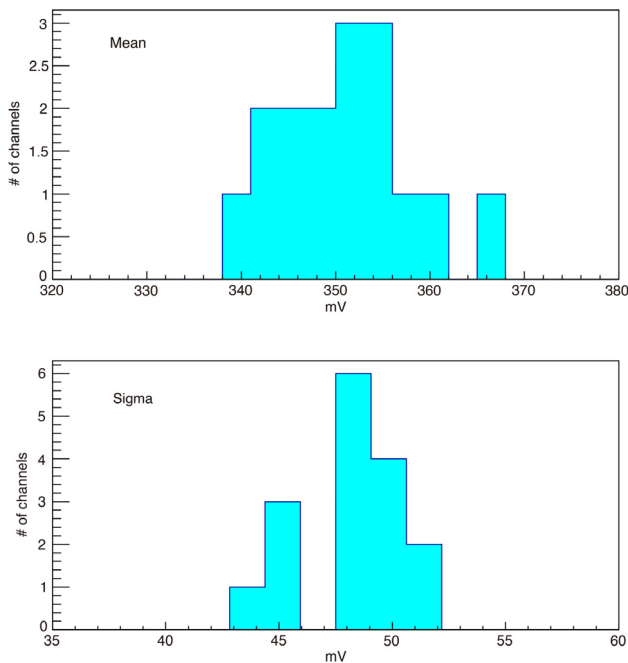


Fig. 12. Top: Mean distribution of the fitted Gaussian function of the 60-keV peak; 351 ± 7 (std) mV. Bottom: Sigma distribution; 48 ± 2 (std) mV.

of ~ 70 ns and a density of 5.4 g cm^{-3} (see Fig. 10). The energy spectra using an ^{241}Am beam for irradiation exhibited distinct peaks at 60 keV, as seen in Fig. 11. Here, the spectra were obtained in the similar manner as the threshold scan as mentioned in Section 4.2 via a coarse shift of the threshold voltage ($\Delta V = 10$ mV). The distributions of the mean and sigma of the fitted Gaussian function for the 60-keV peak are shown in Fig. 12. The variation of the 60-keV peak voltage was within 5% and the average energy resolution of 60 keV (FWHM) for every channel was estimated to be $32\% \pm 1\%$ (std), which ensures the uniform quality of our developed CT array.

5. Discussion and future prospect

In this paper, we presented the development of the LSI (MPPC-CT16) dedicated to the MPPCs for future use in photon-counting CT,

which is first of its kind. The MPPC-CT16 has an ultrafast temporal response capable of counting a current pulse with a high count rate of > 25 MHz/pixel. In addition, it can obtain information on incident X-rays with an energy resolution of 32% (FWHM) at 60 keV through a combination of a 16-channel MPPC array and a 16-channel YGAG array. Furthermore, a superior 16-channel performance has high uniformity, such as a variation of the 60-keV peak voltage within 5%. Here, a significant variation in the pixel performance (e.g., signal gain or energy resolution) leads to degradation of the X-ray image, e.g., the appearance of a ring or streak artifact. Thus, the MPPC-CT16 satisfies the need for uniform performance in CT imaging with a multichannel detector system.

A similar LSI developed for the CZT detector [5] can count X-ray photons up to ~ 60 MHz/mm² by fine pixelation, while our MPPC system, combined with the YGAG scintillators, can count X-ray photons up to ~ 10 MHz/mm² considering the complete pulse timescale of ~ 100 ns. For further improvement of higher-speed photon-counting capability, a faster scintillator should be needed and are currently being developed. The energy resolution of the 60-keV peak is 8% (FWHM) for the CZT system [5], which is much better than that of our MPPC system (32%). However, in our experiment using a single MPPC, we successfully performed K-edge imaging of an iodine phantom using a 33-keV absorption edge [6] and showed that not only CdTe and CZT with their superior energy resolution, but also the MPPC system can offer K-edge imaging. Thus, MPPC-CT16 has great potential to perform K-edge imaging. We will report our results elsewhere.

Acknowledgments

This work was supported by JSPS KAKENHI Grant Number JP15H05720, JP16H07266 and the Key Researchers Development Program at Waseda University.

References

- [1] H. Morita, et al., *Nucl. Instrum. Methods A* 857 (2017) 58–65.
- [2] H. Matsukiyo, et al., *Japan. J. Appl. Phys.* 49 (2R) (2010) 027001.
- [3] P. Shikhaliev, S. Fritz, *Phys. Med. Biol.* 56 (7) (2011) 1905.
- [4] K. Ogawa, et al., *Nucl. Instrum. Methods A* 664 (1) (2012) 29–37.
- [5] R. Steadman, C. Herrmann, A. Livne, *Nucl. Instrum. Methods A* 862 (2017) 18–24.
- [6] H. Morita, et al., (in preparation).